molecules

MDPI

Article

Optical Activity of Chiral Palladium Complexes [Si-O-PdMe(*S*-/*R*-BINAP)] Covalently Bound to Silica Through Grafting

Melanie E. Hoffmann [1], Nathalie Fehn [1], Christoph Gnad [1], Ulrich K. Heiz [1], Klaus Köhler [1,*] and Aras Kartouzian [1,2,*]

[1] Department of Chemistry and Catalysis Research Center, TUM School of Natural Sciences, Technical University of Munich, Lichtenbergstr. 4, 85748 Garching, Germany; melanie.e.hoffmann@tum.de (M.E.H.); natalie.fehn@tum.de (N.F.); ulrich.heiz@mytum.de (U.K.H.)

[2] Helmholtz Zentrum München, Institute of Structural Biology, Ingolstädter Landstr. 1, 85764 Neuherberg, Germany

* Correspondence: klaus.koehler@tum.de (K.K.); aras.kartouzian@tum.de (A.K.)

Abstract

The transfer of molecular chirality to solid surfaces is a focus of research due to its importance for practical applications. While several chiral metal complexes have been anchored to metal oxide surfaces via linkers, the optical properties of those with a direct covalent bond between the metal center and the support's surface oxygen remained unexplored. This study reports the separate synthesis of both enantiomers of palladium(II)-methyl-BINAP complexes (2,2′–Bis(diphenylphosphino)–1,1′–binaphthylmethylpalladium(II)) on silicon dioxide. The precursors [$PdMe_2$(*S*-BINAP)] and [$PdMe_2$(*R*-BINAP)] were synthesized, characterized, and grafted onto partially dehydroxylated SiO_2 to form PdMe(*S*-BINAP)/SiO_2 and PdMe(*R*-BINAP)/SiO_2. Solid-state NMR, infrared spectroscopy, and circular dichroism spectroscopy are consistent with site isolation and the structures of both enantiomerically pure surface complexes. The grafted complexes exhibit mirror-image CD spectra with features distinct from their molecular precursors, indicating that immobilization modifies their chiroptical response. The thermal stability of the surface complexes was studied by temperature-programmed experiments.

Keywords: Palladium; BINAP; grafting; chiral surface complexes; optical activity

1. Introduction

The importance of molecular chirality is well known across different fields of science. Besides the academic interest, several relevant practical applications are directly connected, ranging from chromatography for analytics or separation of enantiomers [1,2] to asymmetric syntheses and catalysis [3–6]. Molecular chirality on solid surfaces plays a distinctive role in both chromatography and heterogeneous enantioselective catalysis, where relevant interactions or reactions take place at the interface of the solid surface and the neighboring phase. In heterogeneous catalysis, several approaches have been used to introduce chirality into solid catalysts [4,7–10]. Practically, the most successful and common standards are the adsorption of a chiral molecule, the modifier, to a well-known and understood achiral solid catalyst [11–13] and the bonding of a chiral, catalytically active metal complex via a linker between the backbone of a chiral ligand and a surface functional group, so-called anchoring [14–16]. In both cases, the aim is to exploit the activity of well-known catalysts,

Check for updates

Academic Editor: Afang Zhang

Received: 29 September 2026
Revised: 5 November 2026
Accepted: 8 November 2026
Published: 11 November 2026

Copyright: © 2026 by the authors. Licensee MDPI, Basel, Switzerland. This article is an open access article distributed under the terms and conditions of the Creative Commons Attribution (CC BY) license.

like supported metal nanoparticles or homogenous catalysts, which will be immobilized in this way. In other words, the chiral precursor should ideally not be changed at all during the immobilization (avoiding any change in the first coordination sphere) in order to keep the catalytic performance and to combine it with enantioselectivity. Chosen reports showed, however, that even the atom of the ligand to which the linker is bound in this second coordination sphere of the complex can clearly change the enantiomeric excess [17].

At least from an academic point of view, it is therefore an interesting question how the chirality of a complex is influenced when the metal complex is not connected to a surface through a linker, but is directly covalently bound to surface atoms, such as the oxygen of an oxide, in its first coordination sphere [18–21]. This kind of immobilization of metal complexes can best be achieved by grafting a suitable precursor via protolysis of the surface hydroxyl groups of the oxide support, an approach known as Surface Organometallic Chemistry (SOMC) [22,23]. For high surface area materials, the best-known and understood is the surface chemistry of silicon dioxide, SiO_2. Looking for an interesting model compound (chiral ligand and catalytically active central metal atom), BINAP (2,2′-Bis(diphenylphosphino)-1,1′-binaphthyl) as a ligand and palladium as the active metal came into consideration for several reasons.

1,1′-Binaphthyl derivatives constitute a group of compounds broadly employed in many chiral recognition processes, in asymmetric organic synthesis and catalysis [11,24]. The chiroptical properties and characterization methods of BINAP have been extensively investigated [25,26], including its adsorption on palladium nanoparticle surfaces [12]. BINAP complexes of ruthenium and palladium have been used mostly as homogeneous but also as heterogeneous catalysts on several supports in an impressive number of asymmetric reactions [15,16,24,27]. The metal complex of palladium and BINAP with two additional methyl ligands, [$PdMe_2$(BINAP)], was the subject of a study on its synthesis and characterization very recently [28]. Both enantiomers of this complex could be synthesized in high purity and characterized structurally by single-crystal X-ray analysis and by spectroscopic methods. This is a good basis for investigations as a model system for the clearly more complex and analytically more demanding surface system. This complex exhibited an interesting additional induced circular dichroism (ICD) effect on the palladium center [28]. The methyl ligands represent a very suitable leaving group for the grafting reaction of this complex with a surface OH group.

This complex has been chosen in the present work for the first synthesis of enantiomerically pure surface complexes PdMe(*R*-BINAP)/SiO_2 and PdMe(*S*-BINAP)/SiO_2 by grafting. By choosing specific reaction conditions, unwanted side reactions such as palladium self-reduction and racemization can be avoided, and isolated complexes covalently bound to the surface oxygen of silica can be synthesized, structurally identified, and characterized. The chiroptical properties of the complex and the changes relative to the precursor complexes were successfully determined.

2. Results and Discussion

2.1. Synthesis and Structural Characterization of PdMe(BINAP) Complexes on SiO_2

Both enantiomerically pure precursor complexes, [$PdMe_2$(*R*-BINAP)] and [$PdMe_2$(*S*-BINAP)], were synthesized according to a literature procedure in high purity [28]. As the noble metal precursor is expected to undergo self-reduction and form palladium particles, the temperature was kept below room temperature throughout the grafting reaction and during storage of the material.

Both enantiomerically pure precursors were immobilized on partially dehydroxylated silicon dioxide ($SiO_2{}^{700}$), which was heated at 700 °C under high vacuum [29]. As reported and demonstrated in the literature, this pre-treatment results in isolated silanol groups

on the surface. These react under carefully chosen conditions with methyl complexes (grafting) to form well-separated palladium-methyl surface complexes (Figure 1) [23,30,31]. Formation of methane during the immobilization of $PdMe_2$(BINAP) was detected by mass spectrometry in the out-stream gas flow attached to the reaction flask. The grafting was performed in toluene at −37 °C for 16 h. The reaction temperature and time were found to be optimal for avoiding palladium self-reduction and cluster formation [32]. PdMe(*R*-BINAP)/SiO_2^{700} (**A**) and PdMe(*S*-BINAP)/SiO_2^{700} (**B**) were obtained as colorless materials after washing and drying under inert conditions. The concentration of the precursor solutions used for grafting was planned to yield an approximately 1 wt% palladium loading. It is practically not possible to achieve exactly the same loading for such experiments, and thus for both enantiomers. Not all surface ≡SiOH groups reacted under these conditions, further supporting the site isolation of the final surface complexes. Elemental Analysis (EA) of the final products confirmed palladium loadings of 0.64 wt% for **A** and 0.90 wt% for **B**.

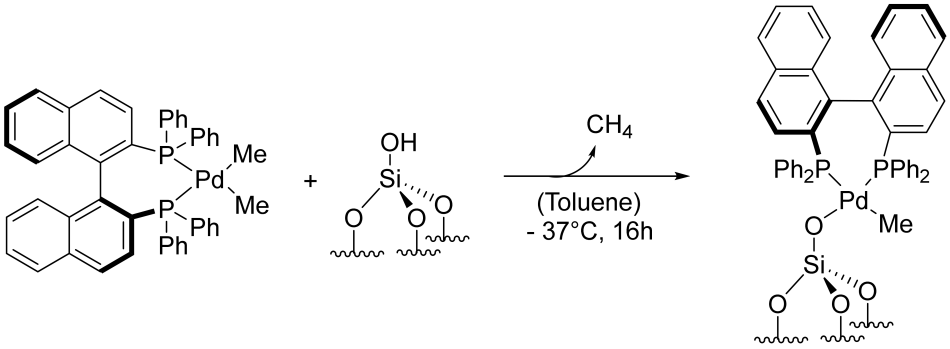


Figure 1. Grafting of $PdMe_2$(*S*-BINAP) onto activated silica (SiO_2^{700}) to achieve a single-site PdMe(*S*-BINAP)/SiO_2^{700} **B** surface complex.

An IR spectrum of a self-supporting disk of **B**, which has been transferred from the glove box to the spectrometer under strictly inert conditions, shows vibrations between 3100 and 2800 cm^{-1}, and between 1500 and 1400 cm^{-1} (Figure 2, red spectrum). As determined by DFT calculations of the precursor complexes [28], the signals around 3100 cm^{-1} can be assigned to stretching vibrations of the phenyl groups of BINAP. The two signals at around 2900 cm^{-1} can be assigned to the C-H stretching of the methyl groups. The additional signal at ~3650 cm^{-1} can be assigned to a disturbed silanol, which is influenced by the proximity of the complex. This effect has already been reported for other surface organometallic frameworks containing aromatic ligands [33,34]. Similar palladium complexes bearing diphenylphosphine ligands show a band at similar frequencies [29]. Further, SiO-H stretching of isolated silanol groups on the surface of silica-700 is observed as the sharp band at 3747 cm^{-1}, indicating that the free silanol groups remained on the silica surface [23]. The IR spectra of the self-supporting disks of **A** and **B** are identical.

The signal for the C-H stretching of the methyl groups declines in intensity compared to free [$PdMe_2$(*S*-BINAP)], as expected for the loss of one methyl group due to the grafting process and supporting the assumption that the palladium complex PdMe(*S*-BINAP)/SiO_2^{700} is bound via one covalent bond to the palladium center. DFT calculations for the PdMe(*S*-BINAP)/SiO_2 surface complex, using -$SiO(OH)_3$ as a model for the silica surface [35], helped assign vibrations to signals in the infrared spectrum (SI). This simplified surrogate, -$SiO(OH)_3$, has previously been shown to be a useful molecular model for calculations.

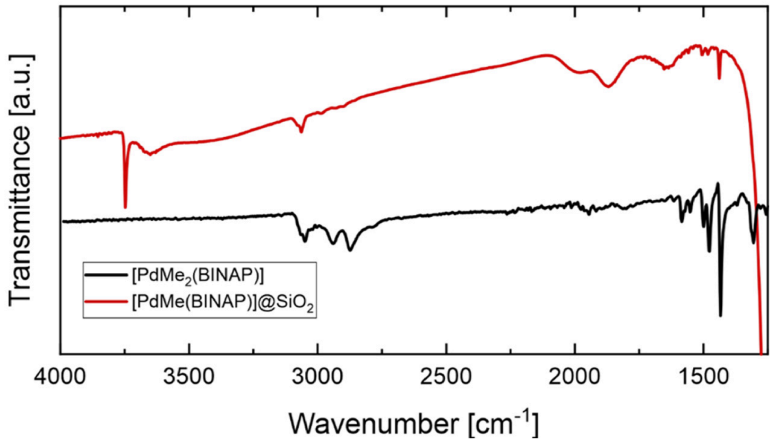


Figure 2. Infra-red spectrum of [PdMe(*S*-BINAP)/SiO_2^{700}]) **B** (red) [$PdMe_2$(*S*-BINAP)] (black).

To further characterize the immobilized complex, solid-state nuclear magnetic resonance spectra (^{1}H-MAS NMR) of samples of both enantiomeric surface complexes, **A** and **B**, were taken. The ^{1}H-MAS NMR of **B** (Figure 3; for **A**, see Figure S3) shows a broad signal at 7.10 ppm for the aromatic protons of the BINAP ligand, an intense peak at 2.14 ppm for the hydroxyl protons of the silica surface, and a signal at 1.25 ppm for the methyl group. These results agree with the expected values. Unfortunately, due to the low palladium loading and the reduced sensitivity to phosphorus nuclei, even long exposure times did not yield well-resolved ^{31}P NMR spectra.

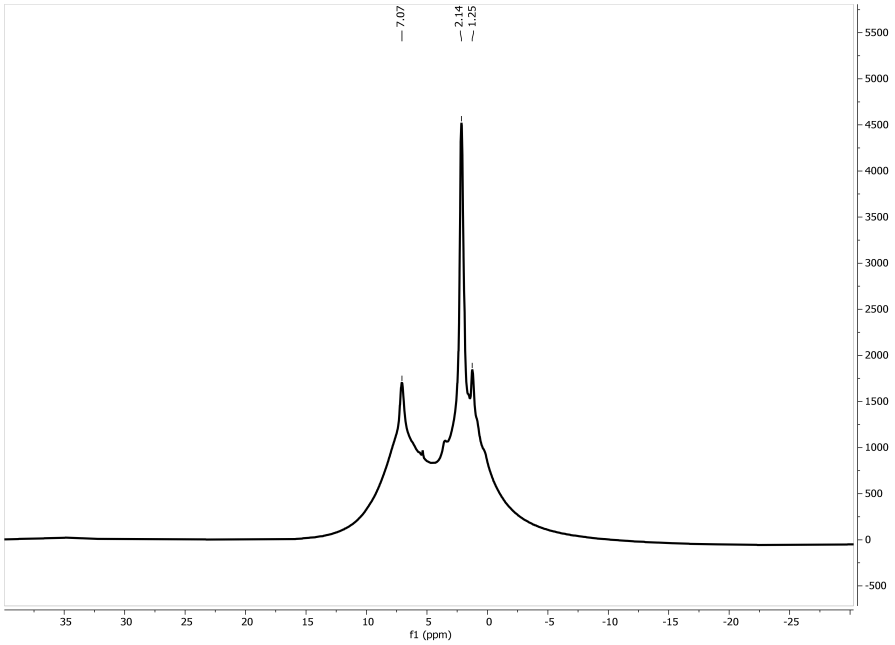


Figure 3. ^{1}H-MAS NMR spectrum of [PdMe(*S*-BINAP)/SiO_2^{700}] **B**.

2.2. Chiroptical Properties of the Surface and the Surface Complexes

The successful synthesis of isolated, structurally well-defined chiral surface complexes with the metal center directly bound to surface oxygens, for the first time, opens the possibility of answering the original questions about changes in chiroptical properties relative to the precursor compounds. Therefore, the chiral solid materials **A** and **B** were suspended in toluene to form transparent gels, and their CD spectra were recorded in comparison to the precursor complexes (Figure 4). The two grafted PdMe(*S*-BINAP)/SiO_2 **B** and PdMe(*R*-BINAP)/SiO_2 **A** are mirror images of each other. While their absorption spec-

tra are essentially identical, their CD responses have opposite signs, as expected for the corresponding enantiomeric surface complexes. The corresponding anisotropy factors, g, which relate the CD response to the respective absorption, are shown in Figure 4A. The two solids show a single band between 350 and 460 nm, with a peak at 400 nm in the CD spectra (Figure 4).

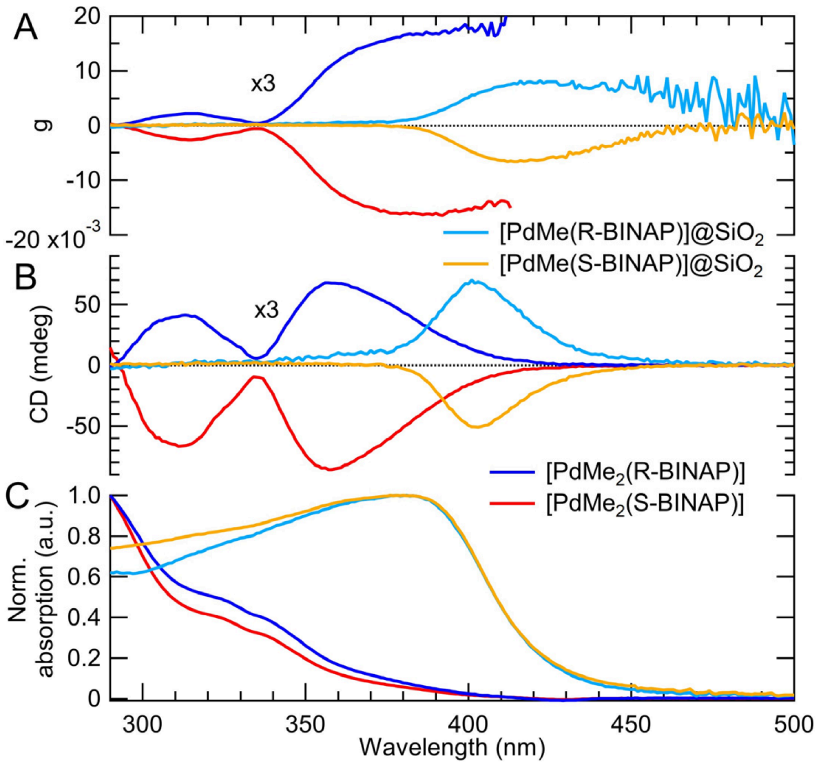


Figure 4. Experimentally obtained anisotropy factor, g (**A**); circular dichroism (**B**); and absorption spectra (**C**) of [$PdMe_2$(*S*-BINAP)], [$PdMe_2$(*R*-BINAP)], PdMe(*S*-BINAP)/SiO_2^{700} **B**, and PdMe(*R*-BINAP)/SiO_2^{700} **A**.

Comparing the CD spectra of the solid materials (grafted complexes) with those of their precursor complexes $PdMe_2$(*S*-BINAP) and [$PdMe_2$(*R*-BINAP)] reveals substantial differences. The prominent bands at 315 nm and 360 nm of the precursor complexes are no longer present. Instead, a band at about 400 nm is observed with the two grafted enantiomers (Figure 4). Since the molecular precursors already exhibit ICD, the changes upon grafting should be interpreted as modifications of their chiroptical response rather than as the emergence of ICD itself. Such modifications may arise from changes in the electronic and geometric environments of the palladium center upon immobilization [36,37]. The present results, however, do not allow the individual contributions of surface-oxygen coordination and other surface-induced effects to be distinguished.

The immobilization of a chiral molecular complex on an oxide surface can modify its local conformation and electronic environment, thereby altering its chiroptical response. Such changes have been reported for chiral molecules and complexes immobilized on silica and other surfaces, where surface interactions can influence the conformation or spatial arrangement of the immobilized species [38–40]. In the present system, the IR spectrum shows a feature at approximately 3650 cm^{-1}, which is consistent with O-H stretching vibrations of silanol groups in a perturbed or structurally distinct environment on the silica surface [33,34].

To eliminate the possibility of linear dichroism [41], the experiment was repeated three times in different cuvettes and orientations, resulting in the same bands. Additionally, a gel of SiO_2-700 in toluene was measured and showed no linear CD signal.

To assess whether molecular precursor complexes remained reversibly associated with the silica surface, CD spectra were recorded from the materials as toluene suspensions. The molecular precursor complexes [Pd(*R*-BINAP)$_2$]/[Pd(*S*-BINAP)$_2$] and [PdMe$_2$(*R*-BINAP)]/[PdMe$_2$(*S*-BINAP)] are soluble in toluene; consequently, weakly or non-covalently associated molecular species would be expected to partition into the liquid phase during suspension. The absence of CD features attributable to the molecular precursor complexes in the suspension spectra therefore provides supporting evidence that the observed chiroptical response predominantly arises from the immobilized material. This observation is consistent with the formation of surface-bound species, although the CD experiment alone does not constitute independent proof of covalent attachment. Similar caution is warranted for CD measurements of particulate materials because light scattering, linear dichroism, and birefringence can contribute to measured CD signals [42–44].

2.3. Stability of the Surface Complexes

For further investigations or applications, it could be interesting to look at the thermal stability and reactivity of the chiral surface complexes. In view of palladium's potential as a hydrogenation catalyst, temperature-programmed experiments in hydrogen were performed.

The samples were heated in a hydrogen gas flow, and gaseous decomposition products were detected by mass spectrometry (Figure S1). Already at room temperature, decomposition of the sample was detected. The mass of methyl steadily increased as the temperature rose. Starting at 50 °C, traces of the BINAP ligand can be detected by mass spectrometry. These results indicate that PdMe(*R*/*S*-BINAP)/$SiO_2{}^{700}$ is unstable under reductive conditions and, unfortunately, not useful for the intended hydrogenation test reactions. This instability contrasts with other site-isolated palladium or platinum surface complexes, which could be stabilized against ligand dissociation, reduction, and agglomeration in the presence of reducing agents, even at clearly elevated temperatures [45–47]. These reports were originally one of the hopes for applications of supported palladium BINAP complexes in catalysis. The BINAP ligand coordinated to surface complexes seems to be sterically too demanding to remain stable and probably also to enable a successful catalytic cycle without ligand dissociation, which is, of course, critical for the enantioselectivity of the reaction. Possibly, higher stability could be expected with the chiral derivative chiraphos as the ligand [48], which incorporates central rather than axial chirality. The alternative, of course, is the linker-based immobilization mentioned earlier for the synthesis of enantioselective catalysts [16].

3. Materials and Methods

3.1. General Handling

Handling and treatment of the dimethyl complexes, $SiO_2{}^{700}$, and the grafted materials were carried out under water-free, inert conditions (Schlenk line, glovebox) and in heat-gun-dried glassware. The precursor and product materials were stored in a freezer (−35 °C), inside the glovebox (MBraun, Labstar Pro, Garching, Germany). The gases argon (purity 5.0, inert gas in the Schlenk line and in the glovebox), helium (purity 4.6), and hydrogen (purity 5.0) were purchased from Westfalen AG, Münster, Germany. These gases were used without further purification. Toluene was delivered as an anhydrous solvent and then degassed by three Freeze-Pump-Thaw cycles. The solvent was then stored over 4 Å molecular sieves.

3.2. Elemental Analysis (EA) of the Grafted Samples

EA was performed as a combustion analysis to determine the carbon and hydrogen contents (Euro EA elemental analyzer, HEKATech GmbH, Haan, Germany). The contents of palladium and phosphorus in the samples were obtained from photometrical analysis by an Agilent Cary 100 UV-vis spectrometer (Santa Clara, CA, USA). Digestion was performed by treating the samples with boiling concentrated sulfuric acid under reduced pressure; the residues were treated with concentrated sulfuric acid, nitric acid, and hydrochloric acid. For quantification, a part of the sample was treated with an ammonium vanadate solution. The resulting phosphate-vanadate was quantified by measuring its absorbance at 410 nm. Palladium was dissolved from the sample by microwave digestion (CEM Discover SP-D, Anton Paar GmbH, Graz, Austria). Its content was determined by Flame Atomic Absorption Spectrometry (F-AAS; Agilent 280FS AA, Santa Clara, CA, USA) at 265.9 nm.

3.3. Infra-Red (IR) Spectroscopy

The solid materials PdMe(*R/S*-BINAP)/$SiO_2{}^{700}$ were pressed into self-supporting pellets (within the glovebox), transferred into a gas-tight IR cell, and then introduced into a Varian 670 FT-IR spectrometer (Agilent, Santa Clara, CA, USA; equipped with a liquid-nitrogen-cooled mercury cadmium telluride (MCT) detector). Typical measurement parameters (depending on the pellet's properties): resolution: 4 cm^{-1}, sensitivity: 8, aperture: 2 cm^{-1}, 25% beam intensity, spectra accumulated by 8 scans at 25 kHz from 700 to 4000 cm^{-1}.

3.4. Solid-State Nuclear Magnetic Resonance (NMR)

The solid-state ^{1}H-MAS-NMR and ^{31}P-HPDEC-NMR spectra were recorded on a Bruker AV 300 NMR spectrometer (Karlsruhe, Germany). Under inert conditions, the solids were placed into a zirconia (ZrO_2) rotor with a 4 mm diameter. They were then sealed inside the glovebox. The spectra were recorded at 303 K, with a rotational frequency of 12 kHz. The measurements were performed at 300 MHz for the ^{1}H spectra and at 122 MHz for the ^{31}P spectra. External standards: (i) adamantane for the ^{1}H spectra (reference signal: ^{1}H, 2.00 ppm), (ii) ammonium hydrogen phosphate (1.11 ppm relative to H_3PO_4) for ^{31}P spectra. The adamantane standard was referred to tetramethylsilane.

3.5. UV-Vis and CD Spectroscopy

For the UV-Vis and CD spectra, the complex samples were dissolved in toluene (0.13 mg/mL), while the grafted complex was suspended in a toluene slurry (30 mg/mL). The solutions/suspensions were placed into 1 mm quartz capillaries and measured at room temperature and under an argon/nitrogen atmosphere using a J-818 spectrometer (JASCO Corporation, Tokyo, Japan) at a scan rate of 50 nm/min, with two to three replicates.

3.6. Synthesis of [$PdMe_2$(S-BINAP)] and [$PdMe_2$(R-BINAP)]

The synthesis of [$PdMe_2$(*S*-BINAP)] and [$PdMe_2$(*R*-BINAP)] was done according to literature procedures [28].

3.7. Grafting of [$PdMe_2$(S-BINAP)] and [$PdMe_2$(R-BINAP)]on $SiO_2{}^{700}$

Fumed silica was pretreated as follows: it was first agglomerated in deionized water, filtered off, and dried at 70 °C for several days. Crushing and sieving yielded a material with grain sizes ranging from 100 to 300 µm. Calcination of the agglomerate in a muffle oven at 500 °C for 8 h (heating rate: 5 $K.min^{-1}$) was followed by partial dehydroxylation at 700 °C for 16 h (heating rate: 2 K min^{-1}). The latter was performed in a quartz Schlenk tube connected to an oil diffusion pump (10^{-5} mbar, Ilmvac 100328, WELCH, Ilmenau,

Germany). After cooling to room temperature, the evacuated flask was transferred into the glovebox. All further handling of the support material, $SiO_2{}^{700}$, must be performed strictly under inert conditions to avoid rehydroxylation [23].

The grafting of the enantiopure complexes [$PdMe_2$(*S*-BINAP)] and [$PdMe_2$(*R*-BINAP)] was done according to the analogous procedure of [$PdMe_2$dppe] previously reported [32]: The desired amount of the dimethyl palladium(II) precursor was dissolved in 5 mL toluene in a Schlenk tube. $SiO_2{}^{700}$ (500 mg, n(SiOH): 0.12 mmol [23]) was suspended in 5 mL of the same solvent in a second flask. The precursor solution was transferred into the suspension of the support material while maintaining a temperature of −37 °C in a cryo-bath. The used tube and cannula were rinsed with an additional 2 mL of solvent. Under occasional shaking and continuous temperature control, the reaction proceeded for 16 h. After filtration of the supernatant, the solid product was washed with fresh toluene (3 × 5 mL), thereby allowing the solvent to soak in for 10 min each time. The colorless solid was dried in vacuo for 10 h, yielding the final products PdMe(*R*-BINAP)/$SiO_2{}^{700}$ (**A**) and PdMe(*S*-BINAP)/$SiO_2{}^{700}$ (**B**).

PdMe(*S*-BINAP)/$SiO_2{}^{700}$ **B**: Elemental analysis (calc.; found) [m%]: C(5.18; 5.49) H(0.39; 0.44) P(0.58; 0.53) Pd(1.0; 0.9) ^{1}H-MAS-NMR (300 MHz, 300 K) δ (ppm) = 7.07 (m, phenyl), 2.14 (s, Si-OH), 1.25 (s, CH_3) IR(pellet): $\tilde{\upsilon}$ = 3747 ($\upsilon_{SiO\text{-}H}$), 3651 ($\upsilon_{SiO\text{-}H}$), 3043 (υ_{phenyl}),2978 (υ_{methyl}), 2895 (υ_{methyl}).

PdMe(*R*-BINAP)/$SiO_2{}^{700}$ **A**: Elemental analysis (calc.; found) [m%]: Pd(1.0; 0.64) ^{1}H-MAS-NMR (300 MHz, 300 K) δ (ppm) = 7.01 (m, phenyl), 1.99 (s, Si-OH), 1.23 (s, CH_3) IR(pellet): $\tilde{\upsilon}$ = 3747 ($\upsilon_{SiO\text{-}H}$), 3649 ($\upsilon_{SiO\text{-}H}$), 3059 (υ_{phenyl}),2987 (υ_{methyl}), 2897 (υ_{methyl}).

3.8. Tracking of Methane Evolution During the Grafting Process by Mass Spectrometry

As a probing experiment to follow the grafting procedure, the out-streaming gas flow was monitored by mass spectrometry (Pfeiffer ThermoStar GSD 320, Asslar, Germany). The methane signal declined after 4 h, indicating that most of the precursor complex has reacted with the surface.

3.9. Temperature-Programmed Reduction in Hydrogen

For a temperature-programmed reduction, a U-shaped glass reactor was charged with 100 mg [PdMe(*S*-BINAP)/$SiO_2{}^{700}$] in the glovebox. The reactor was introduced into analysis systems equipped with a programmable oven and controllable gas feeds. The system was coupled with a quadrupole mass spectrometer (Pfeiffer ThermoStar GSD 320, Asslar, Germany) to detect the decomposition products in the out-stream gas flow. A hydrogen/helium gas flow was supplied to the U-shaped reactor as the temperature increased at 5 K/min. The masses of methyl, BINAP, and phenyl groups were detected at m/z 15, 16, 77, and 78.

3.10. Computational Methods

All calculations were obtained by the Gaussian®16 program [49]. The DFT functional B3LYP was used for all calculations, and two basis sets were considered. The carbon, hydrogen, oxygen, phosphorus, and silicon atoms were calculated using the 6-311++g* basis set. The metal center Pd was calculated using the LanL2DZ split-valence basis set. For this study, the obtained molecules were geometry-optimized, and subsequently, frequency calculations were performed. All calculations were performed on a FUJITSU CELSIUS Workstation with an Intel® Xeon® E-2136 CPU at 3.31 GHz and 64 GB of RAM.

4. Conclusions

The transfer of molecular chirality to solid (oxide) surfaces can be achieved by grafting reactions with suitable precursor complexes. The isolated single-site surface complexes, PdMe(*R*-BINAP)/SiO_2 and PdMe(*S*-BINAP)/SiO_2, were prepared and structurally characterized by infrared spectroscopy, solid-state MAS NMR, and elemental analysis. Unwanted side reactions, such as Pd self-reduction, cluster formation, and ligand dissociation/racemization, could be avoided by careful choice of the reaction conditions. Both enantiomerically pure materials could be investigated by CD spectroscopy. The optical properties of both enantiomerically pure surface complexes are analogous to those of the precursor complexes. Also, the formerly reported induced circular dichroism is indicated. Observed modifications in chiroptical response compared to the precursor complexes may arise from steric limitations at the surface and from the changes in the first palladium coordination sphere due to the covalent bond between Pd and surface oxygen formed by the grafting reaction. Unfortunately, the noble metal surface complexes are not stable under reducing conditions, such as a hydrogen atmosphere, even at only slightly increased temperatures due to self-reduction.

Supplementary Materials: The following supporting information can be downloaded at: https://www.mdpi.com/article/10.3390/molecules31224058/s1, Figure S1: Temperature-programmed desorption/decomposition of PdMe(*S*-BINAP)@$SiO_2{}^{700}$ [0.9 wt%]. The sample was heated with 5 K min^{-1} from rt to 600 °C in a 50 mLmin^{-1} He stream, and the out-streaming gas flow was analyzed by mass spectrometry; Figure S2: IR spectra of [PdMe(*R*-BINAP)]@$SiO_2{}^{700}$ and [PdMe(*S*-BINAP)]@$SiO_2{}^{700}$; Figure S3: ^{1}H-MAS-NMR spectrum of [PdMe(*S*-BINAP)]@$SiO_2{}^{700}$; Table S1: Through DFT, the electronic energy of PdMe(*R*-BINAP) ($SiO(OH)_3$) in Hartree E_h was obtained; Table S2: Through DFT obtained gemoetries of PdMe(*R*-BINAP) ($SiO(OH)_3$); Table S3: Calculated excited states of PdMe(*R*-BINAP)($SiO(OH)_3$), their crossings, rotatory strengths, energies in eV and nm and their oscillator strength; Table S4: Through DFT obtained electronic Energy of PdMe(S-BINAP)($SiO(OH)_3$) in Hartree E_h.; Table S5: Through DFT obtained geometries of [PdMe(*S*-BINAP)($SiO(OH)_3$)]; Table S6: Calculated excited states of [PdMe(*R*-BINAP)($SiO(OH)_3$)], their crossings, rotatory strengths, energies in eV and nm and their oscillator strength.

Author Contributions: Conceptualization, A.K., K.K., and U.K.H.; methodology, M.E.H.; validation, K.K., and A.K.; formal analysis, M.E.H., N.F., and C.G.; investigation, M.E.H., N.F., and C.G.; resources, K.K., and U.K.H.; data curation, M.E.H., and N.F.; writing—original draft preparation, M.E.H.; writing—review and editing, M.E.H., K.K., and A.K.; visualization, M.E.H.; supervision, K.K., A.K., and U.K.H.; project administration, K.K., and A.K.; funding acquisition, A.K. All authors have read and agreed to the published version of the manuscript.

Funding: This research was funded by the TUM Graduate School (TUM-GS) of the Technical University of Munich, by the Deutsche Forschungsgemeinschaft, DFG KA4166/6-1, and the Hans-Böckler Foundation (416387).

Institutional Review Board Statement: Not applicable.

Informed Consent Statement: Not applicable.

Data Availability Statement: All relevant data can be found in this manuscript and in the Supplementary Materials. Further inquiries can be directed to the corresponding authors.

Acknowledgments: The authors thank the TUM Graduate School (TUM-GS) for their support. They would like to thank the analytical laboratory at the Technical University of Munich, Ulrike Ammari, and Petra Ankenbauer, for conducting the elemental analysis. Special gratitude is extended to Gabriele Raudaschl-Sieber for recording the ^{1}H-MAS and ^{31}P-HPDEC spectra. The recording of the first series of CD spectra by Alexander von Weber is acknowledged, too. M.E.H. gratefully acknowledges the financial support from the Hans-Böckler Foundation (416387).

Conflicts of Interest: The authors declare no conflicts of interest.

Abbreviations

The following abbreviations are used in this manuscript:

DFT	Density Functional Theory
BINAP	2,2′-Bis(diphenylphosphino)-1,1′-binaphthyl
CD	Circular dichroism

References

1. Oliveros, L.; Minguillón, C.; Desmazières, B.; Desbène, P.-L. Chiral-bonded silica gel stationary phases obtained from chiral silanes for high-performance liquid chromatography: Comparison of performance with that of stationary phases obtained from γ-aminopropylsilica gel. *J. Chromatogr. A* **1992**, *606*, 9–17. [CrossRef]
2. Barhate, C.L.; Breitbach, Z.S.; Pinto, E.C.; Regalado, E.L.; Welch, C.J.; Armstrong, D.W. Ultrafast separation of fluorinated and desfluorinated pharmaceuticals using highly efficient and selective chiral selectors bonded to superficially porous particles. *J. Chromatogr. A* **2015**, *1426*, 241–247. [CrossRef] [PubMed]
3. Cornils, B.; Herrmann, W.A.; Xu, J.-H.; Zanthoff, H.-W. *Catalysis from A to Z: A Concise Encyclopedia*; John Wiley & Sons: Hoboken, NJ, USA, 2020.
4. Baráth, E. Selective Reduction of Carbonyl Compounds via (Asymmetric) Transfer Hydrogenation on Heterogeneous Catalysts. *Synthesis* **2020**, *52*, 504–520. [CrossRef]
5. Kartouzian, A. Spectroscopy for model heterogeneous asymmetric catalysis. *Chirality* **2019**, *31*, 641–657. [CrossRef] [PubMed]
6. Panagiotopoulou, C.; Anisi, M.; Jeong, C.; Shameli, K.; Alonso-Gómez, J.L.; Kartouzian, A. Engineering Asymmetry: How Chirality Boosts Catalysis, Spin Selectivity, and Light–Matter Interactions. *ChemPhotoChem* **2026**, *10*, e202500386. [CrossRef]
7. McMorn, P.; Hutchings, G.J. Heterogeneous enantioselective catalysts: Strategies for the immobilisation of homogeneous catalysts. *Chem. Soc. Rev.* **2004**, *33*, 108–122. [CrossRef] [PubMed]
8. Hutchings, G.J. HETEROGENEOUS ASYMMETRIC CATALYSTS: Strategies for Achieving High Enantioselection. *Annu. Rev. Mater. Res.* **2005**, *35*, 143–166. [CrossRef]
9. Baiker, A. Crucial aspects in the design of chirally modified noble metal catalysts for asymmetric hydrogenation of activated ketones. *Chem. Soc. Rev.* **2015**, *44*, 7449–7464. [CrossRef] [PubMed]
10. Shukla, N.; Gellman, A.J. Chiral metal surfaces for enantioselective processes. *Nat. Mater.* **2020**, *19*, 939–945. [CrossRef] [PubMed]
11. Reimann, S.; Mallat, T.; Baiker, A. Enantioselective allylic substitution on Pd/Al2O3 modified by chiral diphosphines. *J. Catal.* **2007**, *252*, 30–38. [CrossRef]
12. Reimann, S.; Urakawa, A.; Baiker, A. BINAP adsorption on palladium: A combined infrared spectroscopy and theoretical study. *J. Phys. Chem. C* **2010**, *114*, 17836–17844. [CrossRef]
13. Tamura, M.; Fujihara, H. Chiral bisphosphine BINAP-stabilized gold and palladium nanoparticles with small size and their palladium nanoparticle-catalyzed asymmetric reaction. *J. Am. Chem. Soc.* **2003**, *125*, 15742–15743. [CrossRef] [PubMed]
14. Jones, M.D.; Raja, R.; Thomas, J.M.; Johnson, B.F.; Lewis, D.W.; Rouzaud, J.; Harris, K.D. Enhancing the enantioselectivity of novel homogeneous organometallic hydrogenation catalysts. *Angew. Chem. Int. Ed.* **2003**, *42*, 4326–4331. [CrossRef] [PubMed]
15. Peng, J.; Wang, X.; Zhang, X.; Bai, S.; Zhao, Y.; Li, C.; Yang, Q. Asymmetric hydrogenation by RuCl2 (R-Binap)(dmf) n encapsulated in silica-based nanoreactors. *Catal. Sci. Technol.* **2015**, *5*, 666–672. [CrossRef]
16. Hu, A.; Liu, S.; Lin, W. Immobilization of chiral catalysts on magnetite nanoparticles for highly enantioselective asymmetric hydrogenation of aromatic ketones. *RSC Adv.* **2012**, *2*, 2576–2580. [CrossRef]
17. Choudary, B.; Chowdari, N.S.; Kantam, M.L.; Santhi, P.L. Silica gel anchored chiral Mn (III) salen complexes for enantioselective epoxidation of unfunctionalised olefins. *Catal. Lett.* **2001**, *76*, 213–218. [CrossRef]
18. Conley, M.P.; Copéret, C.; Thieuleux, C. Mesostructured Hybrid Organic–Silica Materials: Ideal Supports for Well-Defined Heterogeneous Organometallic Catalysts. *ACS Catal.* **2014**, *4*, 1458–1469. [CrossRef]
19. Ishizaka, Y.; Arai, N.; Matsumoto, K.; Nagashima, H.; Takeuchi, K.; Fukaya, N.; Yasuda, H.; Sato, K.; Choi, J.C. Bidentate Disilicate Framework for Bis-Grafted Surface Species. *Chemistry* **2021**, *27*, 12069–12077. [CrossRef] [PubMed]
20. Kouhdareh, J. Palladium Schiff Base Complex–Modified Ti (MIL-125) Metal–Organic Frameworks as an Efficient Catalyst for Asymmetric Suzuki Coupling Reactions. *Chirality* **2026**, *38*, e70114. [CrossRef] [PubMed]
21. Ying, T.; Shi, X.; Yan, X.; Lv, H.; Zhu, R.; Zhu, Y.; Wang, Y. Chiral single-atom catalysts for asymmetric synthesis: Intrinsic chiral sites and framework-confinement strategies. *Coord. Chem. Rev.* **2026**, *563*, 218014. [CrossRef]
22. Samantaray, M.K.; Pump, E.; Bendjeriou-Sedjerari, A.; D'Elia, V.; Pelletier, J.D.; Guidotti, M.; Psaro, R.; Basset, J.-M. Surface organometallic chemistry in heterogeneous catalysis. *Chem. Soc. Rev.* **2018**, *47*, 8403–8437. [CrossRef] [PubMed]

23. Copéret, C.; Comas-Vives, A.; Conley, M.P.; Estes, D.P.; Fedorov, A.; Mougel, V.; Nagae, H.; Núñez-Zarur, F.; Zhizhko, P.A. Surface Organometallic and Coordination Chemistry toward Single-Site Heterogeneous Catalysts: Strategies, Methods, Structures, and Activities. *Chem. Rev.* **2016**, *116*, 323–421. [CrossRef] [PubMed]
24. Nieto, S.; Lynch, V.M.; Anslyn, E.V.; Kim, H.; Chin, J. Rapid Identification, Enantiomeric Excess and Concentration Determination Using Simple Racemic Metal Complexes. *Org. Lett.* **2008**, *10*, 5167. [CrossRef] [PubMed]
25. Di Bari, L.; Pescitelli, G.; Salvadori, P. Conformational study of 2, 2 '-homosubstituted 1, 1 '-binaphthyls by means of uv and cd spectroscopy. *J. Am. Chem. Soc.* **1999**, *121*, 7998–8004.
26. Dezhahang, Z.; Merten, C.; Poopari, M.R.; Xu, Y. Vibrational circular dichroism spectroscopy of two chiral binaphthyl diphosphine ligands and their palladium complexes in solution. *Dalton Trans.* **2012**, *41*, 10817–10824. [CrossRef] [PubMed]
27. Dongil, A.B.; Bachiller-Baeza, B.; Guerrero-Ruiz, A.; Rodriguez-Ramos, I. Graphite oxide as support for the immobilization of Ru-BINAP: Application in the enantioselective hydrogenation of methylacetoacetate. *Catal. Commun.* **2012**, *26*, 149–154. [CrossRef]
28. Fehn, N.; Strauss, M.; Jandl, C.; Drees, M.; Heiz, U.; Köhler, K.; Kartouzian, A. On the nature of optical activity in chiral transition metal complexes:[Pd (Me) 2 (BINAP)]. *New J. Chem.* **2023**, *47*, 7961–7964.
29. Gnad, C.; Dachwald, O.; Raudaschl-Sieber, G.; Köhler, K. Synthesis of methyl palladium complexes on silica as single site catalysts activating CCl bonds in heck reactions. *J. Catal.* **2019**, *375*, 257–266. [CrossRef]
30. Rascón, F.; Wischert, R.; Copéret, C. Molecular nature of support effects in single-site heterogeneous catalysts: Silicavs.alumina. *Chem. Sci.* **2011**, *2*, 1449–1456. [CrossRef]
31. Högerl, M.P.; Serena Goh, L.M.; Abou-Hamad, E.; Barman, S.; Dachwald, O.; Pasha, F.A.; Pelletier, J.; Köhler, K.; D'Elia, V.; Cavallo, L.; et al. SOMC grafting of vanadium oxytriisopropoxide ($VO(OiPr)_3$) on dehydroxylated silica; analysis of surface complexes and thermal restructuring mechanism. *RSC Adv.* **2018**, *8*, 20801–20808. [CrossRef] [PubMed]
32. Gnad, C.; Abram, A.; Urstöger, A.; Weigl, F.; Schuster, M.; Köhler, K. Leaching mechanism of different palladium surface species in Heck reactions of aryl bromides and chlorides. *ACS Catal.* **2020**, *10*, 6030–6041. [CrossRef]
33. Allouche, F.; Chan, K.W.; Fedorov, A.; Andersen, R.A.; Copéret, C. Silica-Supported Pentamethylcyclopentadienyl Ytterbium(II) and Samarium(II) Sites: Ultrahigh Molecular Weight Polyethylene without Co-Catalyst. *Angew. Chem.* **2018**, *130*, 3489–3492. [CrossRef]
34. Zhou, H.; Docherty, S.R.; Phongprueksathat, N.; Chen, Z.; Bukhtiyarov, A.V.; Prosvirin, I.P.; Safonova, O.V.; Urakawa, A.; Copéret, C.; Müller, C.R.; et al. Combining Atomic Layer Deposition with Surface Organometallic Chemistry to Enhance Atomic-Scale Interactions and Improve the Activity and Selectivity of Cu–Zn/SiO_2 Catalysts for the Hydrogenation of CO2 to Methanol. *JACS Au* **2023**, *3*, 2536–2549. [CrossRef] [PubMed]
35. Venkatesh, A.; Gioffrè, D.; Atterberry, B.A.; Rochlitz, L.; Carnahan, S.L.; Wang, Z.; Menzildjian, G.; Lesage, A.; Copéret, C.; Rossini, A.J. Molecular and Electronic Structure of Isolated Platinum Sites Enabled by the Expedient Measurement of 195Pt Chemical Shift Anisotropy. *J. Am. Chem. Soc.* **2022**, *144*, 13511–13525. [CrossRef] [PubMed]
36. Noguchi, H.; Takafuji, M.; Maurizot, V.; Huc, I.; Ihara, H. Chiral separation by a terminal chirality triggered P-helical quinoline oligoamide foldamer. *J. Chromatogr. A* **2016**, *1437*, 88–94. [CrossRef] [PubMed]
37. von Weber, A.; Hooper, D.C.; Jakob, M.; Valev, V.K.; Kartouzian, A.; Heiz, U. Circular Dicroism and Isotropy—Polarity Reversal of Ellipticity in Molecular Films of 1,1′-Bi-2-Naphtol. *ChemPhysChem* **2019**, *20*, 62–69. [CrossRef] [PubMed]
38. Ernst, K.-H. Molecular chirality at surfaces. *Physica Status Solidi (b)* **2012**, *249*, 2057–2088. [CrossRef]
39. Linares, M.; Minoia, A.; Brocorens, P.; Beljonne, D.; Lazzaroni, R. Expression of chirality in molecular layers at surfaces: Insights from modelling. *Chem. Soc. Rev.* **2009**, *38*, 806–816. [CrossRef] [PubMed]
40. Muratsugu, S.; Sawaguchi, K.; Shiraogawa, T.; Chiba, S.; Sakata, Y.; Shirai, S.; Baba, H.; Ehara, M.; Akine, S.; Tada, M. Induced chirality at the surface: Fixation of a dynamic M/P invertible helical Co_3 complex on SiO_2. *Chem. Commun.* **2024**, *60*, 2094–2097. [CrossRef] [PubMed]
41. Parrish, K.A.; Salij, A.; Kamp, K.R.; Smith, E.; Utama, M.I.B.; Bergsten, A.J.; Czerwinski, R.; Smith, M.A.; Hersam, M.C.; Poeppelmeier, K.R.; et al. Differential absorption of circularly polarized light by a centrosymmetric crystal. *Science* **2025**, *388*, 1194–1197. [CrossRef] [PubMed]
42. Castiglioni, E.; Biscarini, P.; Abbate, S. Experimental aspects of solid state circular dichroism. *Chirality* **2009**, *21*, E28–E36. [CrossRef] [PubMed]
43. Shindo, Y. On the Problems of CD Spectropolarimeter (IV) Artifacts Due to the Light Scattering by Small Particles. *Appl. Spectrosc.* **1985**, *39*, 713–715. [CrossRef]
44. Ugras, T.J.; Yao, Y.; Robinson, R.D. Can we still measure circular dichroism with circular dichroism spectrometers: The dangers of anisotropic artifacts. *Chirality* **2023**, *35*, 846–855. [CrossRef] [PubMed]
45. Cairns, G.R.; Cross, R.J.; Stirling, D. Characterisation of catalysts and their precursors prepared from supported palladium phosphine complexes. *J. Mol. Catal. A Chem.* **2001**, *172*, 207–218. [CrossRef]

46. Kopietz, L.S.; Schaefer, S.; Storcheva, O.; Raudaschl-Sieber, G.; Bitzer, J.; Kleist, W.; Köhler, K. Silica-Supported Mononuclear Methyl-Platinum Complexes Stabilized by Trimethylphosphine—Synthesis, Structure, and Reactions Under Reducing Conditions. *Chem. A Eur. J.* **2026**, *32*, e71409. [CrossRef] [PubMed]
47. Gnad, C.; Kopietz, L.S.; Bini, C.; Augenstein, H.M.S.; Vummaleti, S.V.C.; Genest, A.; Schaefer, S.; Bitzer, J.; Kleist, W.; Köhler, K. Carbon Monoxide-Induced Mobility of Isolated Palladium Species on Silicon Dioxide at Room Temperature. *Organometallics* **2025**, *44*, 1586–1594. [CrossRef]
48. Fryzuk, M.D.; Bosnich, B. Asymmetric synthesis. Production of optically active amino acids by catalytic hydrogenation. *J. Am. Chem. Soc.* **1977**, *99*, 6262–6267. [CrossRef] [PubMed]
49. Frisch, M.; Trucks, G.; Schlegel, H.; Scuseria, G.; Robb, M.; Cheeseman, J.; Scalmani, G.; Barone, V.; Petersson, G.; Nakatsuji, H. *Gaussian 16, Revision C. 01*; Gaussian. Inc.: Wallingford, CT, USA, 2016.

Disclaimer/Publisher's Note: The statements, opinions and data contained in all publications are solely those of the individual author(s) and contributor(s) and not of MDPI and/or the editor(s). MDPI and/or the editor(s) disclaim responsibility for any injury to people or property resulting from any ideas, methods, instructions or products referred to in the content.